Research Article | Vol. 25, No. 2 | 23 Jan 2017 | OPTICS EXPRESS 799

Optics EXPRESS

Receiver design for SPAD-based VLC systems under Poisson–Gaussian mixed noise model

TIANQI MAO,[1] ZHAOCHENG WANG,[1,*] AND QI WANG[2]

[1]*Tsinghua National Laboratory for Information Science and Technology (TNList), Department of Electronic Engineering, Tsinghua University, Beijing 100084, China*
[2]*School of Electronics and Computer Science, University of Southampton, Southampton SO17 1BJ, UK*
[*]*zcwang@tsinghua.edu.cn*

Abstract: Single-photon avalanche diode (SPAD) is a promising photosensor because of its high sensitivity to optical signals in weak illuminance environment. Recently, it has drawn much attention from researchers in visible light communications (VLC). However, existing literature only deals with the simplified channel model, which only considers the effects of Poisson noise introduced by SPAD, but neglects other noise sources. Specifically, when an analog SPAD detector is applied, there exists Gaussian thermal noise generated by the transimpedance amplifier (TIA) and the digital-to-analog converter (D/A). Therefore, in this paper, we propose an SPAD-based VLC system with pulse-amplitude-modulation (PAM) under Poisson-Gaussian mixed noise model, where Gaussian-distributed thermal noise at the receiver is also investigated. The closed-form conditional likelihood of received signals is derived using the Laplace transform and the saddle-point approximation method, and the corresponding quasi-maximum-likelihood (quasi-ML) detector is proposed. Furthermore, the Poisson-Gaussian-distributed signals are converted to Gaussian variables with the aid of the generalized Anscombe transform (GAT), leading to an equivalent additive white Gaussian noise (AWGN) channel, and a hard-decision-based detector is invoked. Simulation results demonstrate that, the proposed GAT-based detector can reduce the computational complexity with marginal performance loss compared with the proposed quasi-ML detector, and both detectors are capable of accurately demodulating the SPAD-based PAM signals.

OCIS codes: (060.0060) Fiber optics and optical communications; (060.2605) Free-space optical communication; (060.4510) Optical communications.

References and links

1. L. Hanzo, H. Haas, S. Imre, D. C. O'Brien, M. Rupp, and L. Gyongyosi, "Wireless myths, realities, and futures: from 3G/4G to optical and quantum wireless," Proc. IEEE **100**, 1853–1888 (2012).
2. A. Jovicic, J. Li, and T. Richardson, "Visible light communication: opportunities, challenges and the path to market," IEEE Commun. Mag. **51**(12), 26–32 (2013).
3. J. M. Kahn and J. R. Barry, "Wireless infrared communications," Proc. IEEE **85**(2), 265–298 (1997).
4. E. Fisher, I. Underwood, and R. Henderson,"A reconfigurable single-photon-counting integrating receiver for optical communications," IEEE J. Solid-State Circuits **48**(7), 1638–1650 (2013).
5. X. Liu, C. Gong, S. Li, and Z. Xu, "Signal characterization and receiver design for visible light communication under weak illuminance," IEEE Commun. Lett. **20**(7), 1349–1352 (2016).
6. N. Faramarzpour, M. Deen, S. Shirani, and Q. Fang, "Fully integrated single photon avalanche diode detector in standard CMOS 0.18 Îijm technology," IEEE Trans. Electron. Dev. **55**(3), 760–767 (2008).
7. O. Almer, D. Tsonev, N. Dutton, T. Abbas, S. Videv, S. Gnecchi, H. Haas, and R. Henderson, "A SPAD-based visible light communications receiver employing higher order modulation," in *Proceedings of IEEE Global Commun. Conf. (GLOBECOM)* (IEEE, 2015), pp. 1–6.
8. T. Komine, and M. Nakagawa, "Fundamental analysis for visible-light communication system using LED lights," IEEE Trans. Consum. Electron. **50**(1), 100–107 (2004).
9. Y. Li, M. Safari, R. Henderson, and H. Haas, "Optical OFDM with single-photon avalanche diode," IEEE Photon. Technol. Lett. **27**(9), 943–946 (2015).
10. J. Zhang, L. Si-Ma, B. Wang, J. Zhang, and Y. Zhang, "Low-complexity receivers and energy-efficient constellations for SPAD VLC systems," IEEE Photon. Technol. Lett. **28**(17), 1041–1135 (2016).
11. F. Anscombe, "The transformation of Poisson, binomial and negativebinomial data," Biometrika **35**(3–4), 246–254 (1948).

#281409 http://dx.doi.org/10.1364/OE.25.000799
Journal © 2017 Received 23 Nov 2016; revised 3 Jan 2017; accepted 5 Jan 2017; published 10 Jan 2017

Optics EXPRESS

12. D. Chitnis, and S. Collins, "A SPAD-based photon detecting system for optical communications," J. Lightwave Technol. **32**(16), 2028–2034 (2014).
13. Y. Li, S. Videv, M. Abdallah, K. Qaraqe, M. Uysal, and H. Haas, "Single photon avalanche diode (SPAD) VLC system and application to downhole monitoring," in *Proceedings of IEEE Global Commun. Conf. (GLOBECOM)* (IEEE, 2014), pp. 2108–2113.
14. J. Frechette, P. Grossmann, D. Busacker, G. Jordy, E. Duerr, K. McIntosh, D. Oakley, R. Bailey, A. Ruff, M. Brattain, J. Funk, J. MacDonald, and S. Verghese, "Readout circuitry for continuous high-rate photon detection with arrays of InP Geiger-mode avalanche photodiodes," Proc. SPIE **8375**, 83750W (2012).
15. K. Doris, A. Roermund, and D. Leenaerts, *Wide-Bandwidth High Dynamic Range D/A Converters (The Springer International Series in Engineering and Computer Science Series)* (Springer, 2006).
16. Z. Cheng, X. Zheng, D. Palubiak, M. Deen, and H. Peng, "A comprehensive and accurate analytical SPAD model for circuit simulation," IEEE Trans. Elec. Dev. **63**(5), 1940–1948 (2016).
17. J. Starck, F. Murtagh, and A. Bijaoui, *Image Processing and Data Analysis* (Cambridge University, 1998).
18. Y. Li, M. Safari, R. Henderson, and H. Haas, "Nonlinear distortion in SPAD-based optical OFDM systems," in *Proceedings of IEEE Global Commun. Conf. Workshops (GC Wkshps)* (IEEE, 2015), pp. 1–6.
19. C. Helstrom, "Approximate evaluation of detection probabilities in radar and optical communications," IEEE Trans. Aerosp. Electron. Syst. **14**(4), 630–640 (1978).
20. D. Snyder, C. Helstrom, A. Lanterman, M. Faisal, and R. White, "Compensation for readout noise in CCD images," J. Opt. Soc. Am. A **12**(2), 272–283 (1995).

1. Introduction

Visible light communication (VLC) has become a promising technology complement to the radio-frequency (RF) counterpart due to its unlicensed spectrum, high security and safety to human health [1, 2]. In a typical VLC system, light-emitting diode (LED) and photodiode (PD) are utilized at the transmitter and the receiver, respectively. Since the low-cost intensity modulation with direct detection (IM/DD) is often applied in VLC [3], the signals transmitted by LEDs are constrained to be non-negative and real-valued. Currently, the high-speed integrated optical detectors such as avalanche photodiode (APD) are widely employed in VLC systems [4]. However, these detectors are not applicable in the scenarios of weak illuminance or long-distance transmission where the received optical power is relatively low [5].

To address the aforementioned issue, the single-photon avalanche diode (SPAD) [4, 6] is employed for weak optical signal detection, where the reverse bias voltage is different from classical APDs, causing it to operate in Geiger mode instead of linear mode. In comparison with the classical APD, SPAD is more sensitive to optical signals, and can be employed as a photon counter. Due to interference sources such as the dark current, there exists Poisson-distributed noise at the SPAD receiver [6, 7]. Unlike APD-based VLC systems, where the additive white Gaussian noise (AWGN) channel is assumed [8], the conventional detection scheme cannot be directly adopted in the SPAD-based VLC systems. In [9], the optical orthogonal frequency division multiplexing (O-OFDM) using the SPAD is proposed, where the DC-based optical OFDM (DCO-OFDM) and the asymmetrically clipped optical OFDM (ACO-OFDM) are considered. Whilst in [10], the SPAD-based VLC system with pulse-amplitude-modulation (PAM) is investigated, and the Anscombe root transform [11] is employed for demodulating the Poisson-distributed signals. Moreover, [12] illustrates the SPAD hardware design in optical communications.

In [4, 9, 10, 13], the digital SPAD is employed for photon detection, where a digital counter is used to generate discrete outputs. Therefore, the receiver is not influenced by the Gaussian thermal noise. However, as is discussed in [4, 12, 14], for digital SPADs, the counting process is required to be precisely synchronized to the transmitter clock, and additional receiver design work is necessary for recovering the clock and the data from transmitted signals, which may lead to degradation of the system performance and increased overhead at the receiver. Due to this clock synchronization issue of the digital SPAD, the analog SPAD without the counter is considered in this paper, where equally weighted current steering digital-to-analog converters (D/A) [12, 15] are employed to generate current signals, and a transimpedance amplifier

Optics EXPRESS

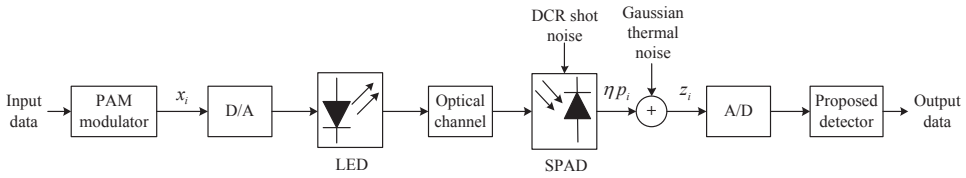

Fig. 1. SPAD-based PAM system model.

(TIA) is optionally applied to enhance the bandwidth. Therefore, there exists additive Gaussian thermal noise [12, 16], which distorts the output signal of the SPADs. In this paper, the Poisson-Gaussian (P-G) mixed noise model is investigated in the SPAD-based PAM system. Due to P-G mixed noise, the statistical characteristic is changed and the traditional receivers in the existing literature cannot work well. In this work, the approximate closed-form conditional likelihood of received signals is derived using the Laplace transform and the saddle-point approximation, and the corresponding quasi-maximum likelihood (ML) detector is proposed. To reduce the computational complexity, the generalized Anscombe transform (GAT) is invoked for the pre-distortion of the noisy signals [17]. The predistorted signal becomes Gaussian distributed with unity variance, yielding an equivalent AWGN channel. Therefore, a reduced-complexity GAT-based detector with hard decision is proposed, where the corresponding decision thresholds are formulated. In simulations, due to the low output rate of the SPAD [4], an SPAD array consist of enormous diodes used in [4] is adopted to enhance the output rate. Numerical results demonstrate that the reduced-complexity GAT-based detector only suffers negligible performance loss compared with the quasi-ML detector. It is also indicated that both the proposed quasi-ML detector and the GAT-based detector outperform the conventional ML detector and the hard-decision-based detector in [10], which demonstrates their capability of accurately demodulating the SPAD-based PAM signals.

The remainder of the paper is organized as follows. Section 2 describes the SPAD-based PAM system model with the P-G mixed noise. Section 3 proposes the quasi-ML detector and the reduced-complexity GAT-based detector and presents the corresponding formula derivations. The performances of two proposed detectors are evaluated via Monte Carlo simulations in Section 4, using the conventional detectors for the Poisson noise model [10] as benchmarks. And the conclusion is drawn in Section 5.

2. System model

The system model of the SPAD-based PAM system is illustrated in Fig. 1. At the transmitter, K binary bits are firstly partitioned into blocks. Each block of $\log_2 M$ bits is modulated into a unipolar M-PAM symbol, which is included in the constellation set $\mathbf{C} = \{C_0, C_1, \cdots, C_{M-1}\}$. The resultant real-valued symbols $\mathbf{x} = [x_0, x_1, \cdots, x_{N-1}]$ where $N = K/\lfloor \log_2 M \rfloor$ are then fed into a digital-to-analog converter (D/A), and the output signals can be directly injected into the LED emitter.

At the receiver, the optical signals are detected by the SPAD, and the photon counts are converted into current signals proportionally by the D/A, which then transmitted to the next stages of the receiver. Since the SPAD needs to be recharged after an avalanche is triggered by the arrived photons, during which photon counting is unavailable, the measured mean value of the photon counts suffers from nonlinear distortion, and the recharging time is defined as dead time (DT) [18]. In this paper, however, it is assumed that the time period to detect a photon is much longer than the DT so that its effect could be negligible [9, 10, 13]. Moreover, aside from the Poisson-distributed noise in the SPAD, the system performance is also influenced by the

Optics EXPRESS

Gaussian-distributed thermal noise generated by the subsequent stages of the receiver including the TIA and D/A. Hence, the channel model can be represented as

$$z_i = \eta p_i + n_i, \quad i = 0, 1, \cdots, N-1, \tag{1}$$

where z_i represents the received current signal, η denotes a photon-count-to-current converting factor, n_i follows $\mathcal{N}(0, \sigma^2)$, and p_i denotes the output photon counts with Poisson noise, which can be modeled as a Poisson variable with its mean given by

$$\lambda_i = (QT/E)x_i + N_d T = \alpha x_i + \beta, \tag{2}$$

where Q denotes the photon detection efficiency, N_d stands for the dark count rate (DCR) of the SPAD, E represents the photon energy, and T is defined as the time period to detect a photon. Hence, the PDF of p_i can be formulated as

$$Pr(p_i = n|\lambda_i) = e^{-\lambda_i}\frac{\lambda_i^n}{n!}. \tag{3}$$

According to Eqs. (1) and (3), the conditional likelihood of the variable z_i can be described as

$$p(z_i|\lambda_i, \sigma) = \sum_{n=0}^{+\infty}\left(\frac{\lambda_i^n e^{-\lambda_i}}{n!} \times \frac{1}{\sqrt{2\pi\sigma^2}}\exp\left(-\frac{(z_i - n)^2}{2\sigma^2}\right)\right). \tag{4}$$

Based on the aforementioned statistical properties of received signals, two low-complexity detectors including a quasi-ML detector and a GAT-based detector are proposed for demodulation, which will be discussed in the next section.

3. The proposed detectors

3.1. Low-complexity quasi-ML detector

Since the conditional likelihood of the signal z_i has been formulated in Eq. (4), the ML criterion can be employed for signal demodulation, which is

$$\hat{x}_{bias} = \arg\max_{\hat{x}_i \in \mathbf{C}} \{p(z_i|\alpha\hat{x}_i + \beta, \sigma)\}, \tag{5}$$

However, it can be observed from Eq. (4) that the expression of $p(z_i|\lambda_i, \sigma)$ is too complex to be implemented, since the sum of infinite series has to be calculated. In this paper, we propose an approximate closed-form conditional likelihood for a simplified ML detector.

By performing the Laplace transform on $p(z_i|\lambda_i, \sigma)$, we have

$$\mathcal{L}\{p(z_i|\lambda_i, \sigma)\}(s) = \int_{-\infty}^{+\infty} p(x|\lambda_i, \sigma)e^{-sx}dx = \exp\left(\lambda_i\left(e^{-s} - 1\right) + 0.5\sigma^2 s^2\right). \tag{6}$$

Then the inverse Laplace transform is applied to $\mathcal{L}\{p(z_i|\lambda_i, \sigma)\}(s)$, which yields

$$p(z_i|\lambda_i, \sigma) = \frac{1}{2\pi j}\int_{c-j\infty}^{c+j\infty}\exp\left(f(s)\right)ds, \tag{7}$$

where $f(s) = z_i s + 0.5\sigma^2 s^2 + \lambda_i\left(e^{-s} - 1\right)$. After that, we employ the saddle-point approximation methods [19, 20] to obtain the approximate closed-form expression of the conditional likelihood, which can be formulated as

$$p(z_i|\lambda_i, \sigma) \approx \frac{1}{\sqrt{(2\pi f''(\hat{s}))}}\exp\left(f(\hat{s})\right), \tag{8}$$

Optics EXPRESS

where

$$f''(s) = \frac{\partial^2 f(s)}{\partial s^2} = \lambda_i e^{-s} + \sigma^2, \tag{9}$$

and the saddle point $\hat{s}$ can be calculated by solving the following equation

$$f'(\hat{s}) = z_i + \sigma^2 \hat{s} - \lambda_i \exp(-\hat{s}) = 0. \tag{10}$$

Since Eq. (10) is a nonlinear equation, the Newton-Raphson iteration method is employed for accurate estimation of $\hat{s}$, which can be represented as

$$\hat{s}_{new} = \hat{s}_{pre} - \frac{z_i + \sigma^2 \hat{s}_{pre} - \lambda_i e^{-\hat{s}_{pre}}}{\sigma^2 + \lambda_i e^{-\hat{s}_{pre}}}, \tag{11}$$

where $\hat{s}_{pre}$ and $\hat{s}_{new}$ denote the root of Eq. (10) obtained in the previous iteration and the present iteration, respectively. More specifically, we have the following approximation

$$\exp(\hat{s}) \approx 1 - \hat{s}, \quad -1 < \hat{s} < 1, \tag{12}$$

and the initial value of $\hat{s}$ for Newton-Raphson iterations can be derived by applying Eq. (12) to Eq. (10) as

$$\hat{s}_0 = \frac{\lambda_i - z_i}{\lambda_i + \sigma^2}. \tag{13}$$

By using the aforementioned derivations of $p(z_i|\lambda_i, \sigma)$, the ith transmitted symbol can be detected by our proposed ML-based receiver as

$$\begin{aligned} \hat{x}_i &= \arg\max_{\hat{x}_i \in \mathbf{C}} \{p(z_i|\alpha\hat{x}_i + \beta, \sigma)\} \\ &= \arg\max_{\hat{x}_i \in \mathbf{C}} \left\{ \frac{1}{\sqrt{(2\pi f''(\hat{s}))}} \exp\left(f(\hat{s})\right) \right\}. \end{aligned} \tag{14}$$

It can be seen from Eq. (14) that, the proposed quasi-ML detector only needs to deal with a relatively simple closed-form likelihood without complex operations such as calculating the sum of infinite series, which reduces the computational complexity of the conventional counterpart in Eq. (4). However, the proposed detector is still complicated, since it has to solve the nonlinear equation Eq. (10) for every possible transmitted symbol in $\mathbf{C}$ to calculate the conditional likelihood.

3.2. GAT-based detector

To further reduce the computational complexity, we propose a GAT-based detector with hard decision. The GAT can be formulated as

$$T(z_i) = \begin{cases} 2\sqrt{z_i + 0.375 + \sigma^2}, & z_i + 0.375 + \sigma^2 > 0; \\ 0, & z_i + 0.375 + \sigma^2 \leq 0. \end{cases} \tag{15}$$

According to [17], by applying the GAT to P-G distributed signals, the resultant outputs can be approximately modeled as Gaussian variables with unity variance, which is described as

$$T(z_i) = E\{T(z_i)|\lambda_i, \sigma\} + n_i', \tag{16}$$

where $E\{\cdot\}$ stands for the expectation operator, and n_i' is an AWGN component following $\mathcal{N}(0, 1)$. Therefore, we only need to detect the signal $e_i = E\{T(z_i)|\lambda_i, \sigma\}$ for $i = 0, 1, \cdots, N-$

Optics EXPRESS

Algorithm 1 The proposed GAT-based detector for PAM systems using SPAD

Require: the GAT of the i-th received signal $T(z_i)$, the decision thresholds $\mathbf{D}$, and the constellation set $\mathbf{C}$;

Ensure: $\hat{x}_i$ is the estimation of the i-th transmitted symbol;

```
if T(z_i) < D_0 then
    x̂_i = c_0;
    return x̂_i;
end if
if T(z_i) > D_{M-2} then
    x̂_i = c_{M-1};
    return x̂_i;
end if
for (j = 1; j ≤ M − 2; j++) do
    if D_{j-1} ≤ T(z_i) ≤ D_j then
        x̂_i = c_j;
        return x̂_i;
    end if
end for
```

1 under an AWGN channel. To obtain the decision thresholds for the detector, the expression of e_i is formulated as

$$e_i = \int_{-\infty}^{+\infty} T(z_i) p(z_i|\lambda_i, \sigma) dz_i. \tag{17}$$

By applying the aforementioned saddle-point approximation, Eq. (17) can be further derived as

$$e_i \approx \int_{-\infty}^{+\infty} T(z_i) \frac{1}{\sqrt{2\pi f''(\hat{s}_i)}} \exp\{f(\hat{s}_i)\} dz_i, \tag{18}$$

where $z_i = \lambda_i \exp(-\hat{s}_i) - \sigma^2 \hat{s}_i$. Thus we have

$$e_i \approx \int_{-\infty}^{u_i} 2\sqrt{\lambda_i e^{-\hat{s}_i} - \sigma^2 \hat{s}_i + 0.375 + \sigma^2} \times \exp\left\{\lambda_i (e^{-\hat{s}_i} s + e^{-\hat{s}_i} - 1)\right\} \sqrt{\frac{\lambda_i e^{-\hat{s}_i} + \sigma^2}{2\pi}} d\hat{s}_i, \tag{19}$$

where u_i is the solution of the equation

$$\Phi(\lambda_i, u_i) = \lambda_i \exp(-u_i) - \sigma^2 u_i + 0.375 + \sigma^2 = 0. \tag{20}$$

Define $g(c_i)$ as the function of c_i that has the same form of Eq. (19) but replaces the received noisy signal z_i by c_i $(0 \le i \le M-1)$, which can be represented as

$$g(c_i) = \int_{-\infty}^{u_i'} 2\sqrt{\lambda_i' e^{-s} - \sigma^2 s + 0.375 + \sigma^2} \times \exp\left\{\lambda_i' (e^{-s} s + e^{-s} - 1)\right\} \sqrt{\frac{\lambda_i' e^{-s} + \sigma^2}{2\pi}} ds, \tag{21}$$

where $\lambda_i' = \alpha c_i + \beta$, and u_i' denotes the solution of $\Phi(\lambda_i', u_i') = 0$. Then the sequence $\mathbf{G} = [g(c_0), g(c_1), \cdots, g(c_{M-1})]$ is utilized to calculate $(M-1)$ decision thresholds $\mathbf{D} = [D_0, D_1, \cdots, D_{M-2}]$ as

$$D_i = (g(c_i) + g(c_{i+1}))/2, i = 0, 1, \cdots, M-2. \tag{22}$$

Optics EXPRESS

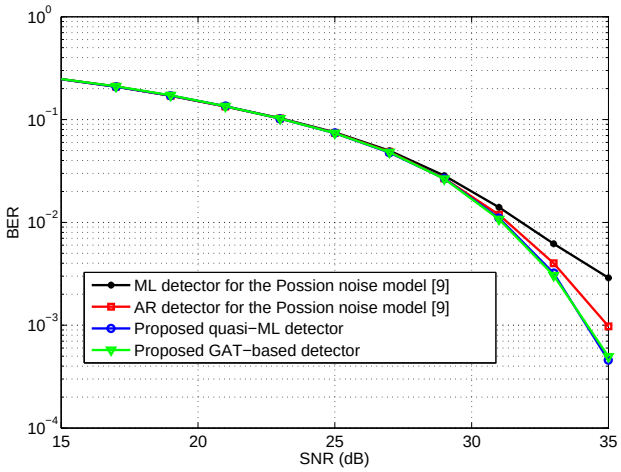

(a) Performance comparison using 16-PAM.

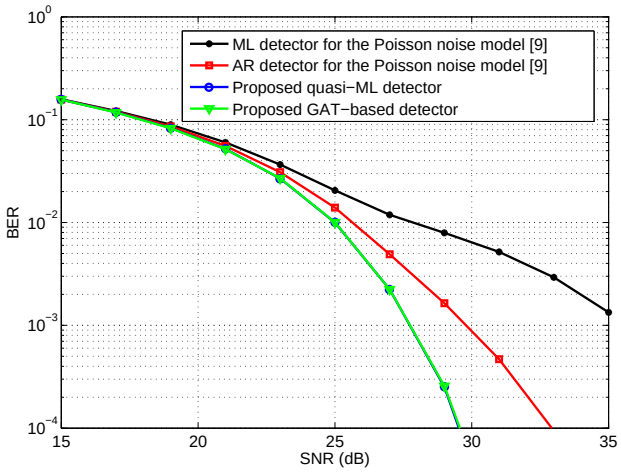

(b) Performance comparison using 8-PAM.

Fig. 2. Performance comparison between the proposed quasi-ML detector, the GAT-based detector, and the receivers illustrated in [10] (this graph shows the BER of each receiver versus SNR of the Gaussian component whilst the noise in the Poisson component is constant due to the fixed optical irradiance of −70dBm, where the average photon count equals 4.5×10^4).

Optics EXPRESS

The proposed GAT-based detector can be illustrated by Algorithm 1. For the proposed GAT-based detector, although the decision thresholds are calculated by solving Eq. (20) and performing integration for every c_i for $i = 0, 1, \cdots, M-1$, it can be neglected in the complexity analysis, since we only need to calculate the decision thresholds for one time before the hard decision of received signals. Therefore, the complexity for the proposed GAT-based detector is on the order of $O(M/2)$. Whilst for the proposed quasi-ML detector, assuming that the number of required operations to calculate the conditional likelihood of each c_i is F, then the complexity of the proposed quasi-ML detector is on the order of $O(FM)$. Hence, It is indicated that the GAT-based detector is capable of reducing the computational complexity compared with the quasi-ML detector.

4. Simulation results

To demonstrate the feasibility of the proposed quasi-ML detector and the reduced-complexity GAT-based detector, their BER performances are compared with the conventional ML detector and the Anscombe root (AR) detector for the Poisson noise model in [10] under the P-G mixed noise model. In simulations, the photodiode and quenching part of the SPAD array introduced in [4] is employed together with the equally weighted current steering readout circuit in [12], which constitutes an analog SPAD detector. Therefore, the values of α and β are set as 4.52×10^{14}s/J and 7.27 [4, 10], and η is equal to 1amp (A) without loss of generality. Moreover, the DT and the bit time are set as 13.5ns and 1ms [4, 10], which indicates that the effect of DT is negligible, since it is smaller than the bit time by 5 orders of magnitude. Note that an optimal constellation alphabet SPAM is proposed in [10]. Although it outperforms PAM when only the Poisson noise is considered, the conventional PAM presents its superiority over SPAM when the Gaussian noise is non-negligible. Therefore, 16-PAM and 8-PAM are adopted in this paper.

The BER performances of the SPAD-based PAM systems with the proposed quasi-ML and GAT-based detectors at the optical irradiance of -70dBm are presented in Fig. 2, using the conventional counterparts for the Poisson noise model in [10] as benchmarks. In Fig. 2, the term SNR denotes the signal-to-noise power ratio of the Gaussian thermal noise. For different orders of constellations, it can be seen that the performances of the two proposed detectors and the conventional receivers are almost the same at low SNRs. This is mainly due to the fact that the noise energy is too large for accurate detection, causing the corresponding BER values to be above 10^{-2}. In high SNR regions, there is negligible difference between the performances of the proposed GAT-based detector and quasi-ML detectors. Since the computational complexity of the proposed GAT-based detector is significantly reduced, it is more attractive in practical SPAD-based PAM systems. Moreover, at the BER of 10^{-3}, the proposed quasi-ML and GAT-based detectors attain about 1dB and 2.5dB performance gain over the conventional AR detector with 16-PAM and 8-PAM respectively, since AR detector neglects the effect of Gaussian noise.

Besides, for both 16-PAM and 8-PAM, the two proposed detectors achieve more than 5 dB performance enhancement over the conventional ML detector in [10] when the BER equals 10^{-3}, for the reason that the likelihood function used in [10] is inaccurate for the P-G mixed noise model. Note that the conventional AR detector presents better BER performance than the conventional ML detector at high SNRs, since the output signals of the AR transform becomes closer to Gaussian variables for low Gaussian noise energy.

In Fig. 3(a) and 3(b), the performances of two proposed detectors and their conventional counterparts described in [10] are simulated with respect to the optical irradiance at the SNR of 35dB and 30dB for 16-PAM and 8-PAM respectively. For different modulation schemes, the conventional AR detector suffers from performance loss compared with two proposed detectors at the BER of 10^{-3}, and the conventional quasi-ML detector performs even worse, since the signals after performing the AR transform cannot be approximated as Gaussian variables, and the conditional likelihood of the conventional quasi-ML detector is inaccurate for the P-G mixed noise

Optics EXPRESS

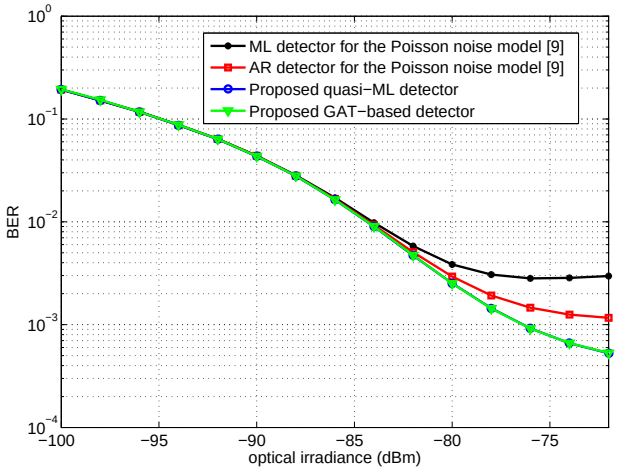

(a) Performance comparison using 16-PAM at the SNR of 35dB.

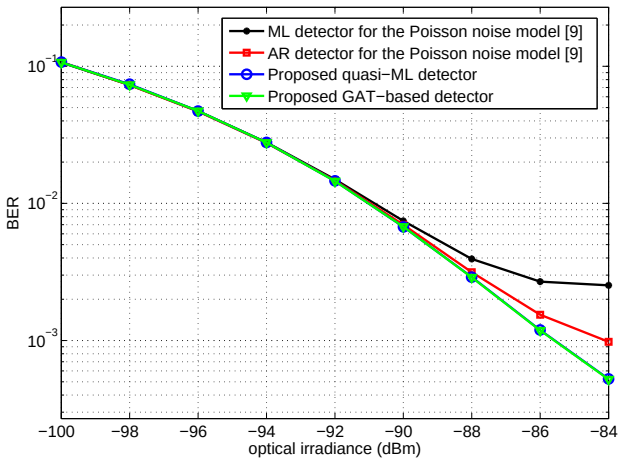

(b) Performance comparison using 8-PAM at the SNR of 30dB.

Fig. 3. Performance comparison between the proposed quasi-ML detector, the GAT-based detector, and the receivers illustrated in [10] with respect to the optical irradiance.

Optics EXPRESS

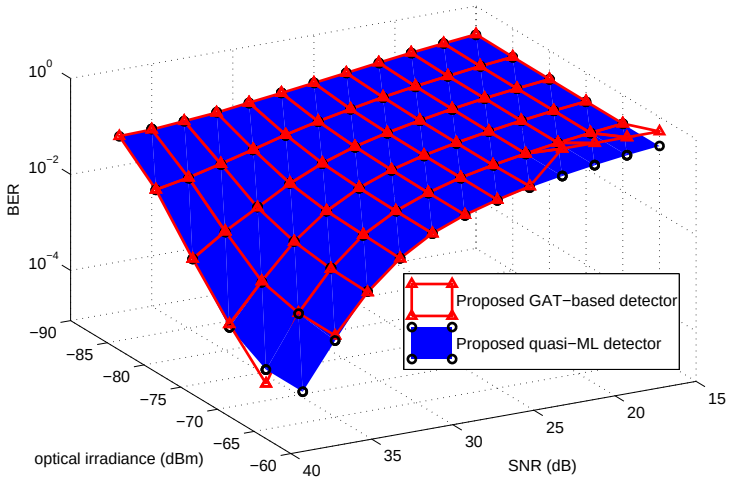

Fig. 4. Performance comparison between the SPAD-based VLC systems with the proposed quasi-ML detector and the GAT-based detector.

model. Therefore, it is indicated that the conventional detectors are no longer applicable under the P-G mixed noise model. In contrast, the proposed quasi-ML and the GAT-based detectors are capable of detecting the PAM signals accurately, which achieve the significant performance gain over the conventional counterparts at the BER of 10^{-3}.

Figure 4 presents the performance comparison between the proposed quasi-ML and GAT-based detectors, where 16-PAM is employed. It can be seen that the BER value decreases as the SNR and the optical irradiance become high. Moreover, despite the slight performance gap between the proposed quasi-ML and GAT-based detectors at low SNRs, the performances of the two detectors are almost the same. It demonstrates the superiority of the proposed GAT-based detector over the quasi-ML detector, since its computational complexity is reduced with negligible performance loss.

5. Conclusions

In this paper, the P-G mixed noise model is investigated in the SPAD-based PAM system, where the analog SPAD detector [12] is applied. The corresponding quasi-ML detector and reduced-complexity GAT-based detector with hard decision are proposed. For quasi-ML detection, the closed-form expression for the conditional likelihood of received signals is derived with the aid of the Laplace transform and the saddle-point approximation, which reduces the computational complexity considerably. For GAT-based detection, the resultant signals after performing GAT on received P-G distributed signals can be approximated as Gaussian variables. Thus the reduced-complexity hard-decision detector could be employed. Simulation results validate that the proposed ML and GAT-based detectors outperform their conventional counterparts, and are capable of detecting SPAD-based PAM signals accurately under the P-G mixed noise model. Besides, it is also demonstrated that the proposed GAT-based detector could reduce the computational complexity with negligible performance degradation compared with quasi-ML detection.

Optics EXPRESS

In this paper, we restrict our work on the receiver design of the SPAD-based PAM system under the P-G mixed noise model, where the effects of DT are neglected. In fact, there are two scenarios of different DT lengths for the SPAD-based PAM system under the P-G mixed noise model: when the bit time is much smaller than DT, the SPAD can be modeled as a photon counter under the P-G mixed noise; when the bit time is comparable with DT, the SPAD cannot be modeled with P-G characteristics, and the nonlinearity of DT should be considered. Therefore, in the future study, the nonlinear transfer characteristics of DT will be also investigated in the SPAD-based PAM system, and the original transceiver design should be modified to combat the nonlinear distortions caused by DT. Moreover, experiments based on hardware will be performed to further validate our contributions.

Funding

National Key Basic Research Program of China (2013CB329200); Shenzhen Subject Arrangements (JCYJ20160331184124954); Shenzhen Peacock Plan (1108170036003286); Guangdong Science and Technology Planning Project (2014B010120001); Shenzhen Fundamental Research Project (JCYJ20150401112337177); Shenzhen Visible Light Communication System Key Laboratory (ZDSYS20140512114229398); EPSRC funded projects (EP/N004558/1, EP/N023862/1).